applied sciences

MDPI

*Article*

# Synthesis and Utilisation of Hybrid Metal-Carbonic Anhydrase Enzyme Carrier System for Soil Biocementation

**Wilson Mwandira [1], Diane Purchase [2], Maria Mavroulidou [1,*] and Michael J. Gunn [1]**

[1] Division of Civil and Building Services Engineering, London South Bank University, 103 Borough Road, London SE1 0AA, UK; mwandiw2@lsbu.ac.uk (W.M.); gunnm@lsbu.ac.uk (M.J.G.)
[2] Department of Natural Sciences, Middlesex University, The Burroughs, London NW4 4BT, UK; d.purchase@mdx.ac.uk
* Correspondence: mavroum@lsbu.ac.uk; Tel.: +44-2078157646

**Abstract:** Biocementation is an emerging nature-inspired method of producing eco-friendly cement for soil stabilization. This paper used the bovine-derived carbonic anhydrase (CA) enzyme to catalyse the bioprecipitation of $CaCO_3$ in a fine-grained soil and thus to biocement the soil. To increase the efficiency of the CA, an innovative copper–carbonic anhydrase (CA) hybrid was fabricated. This study is a proof-of-concept of the potential application of these enzyme carriers for soil biocementation. The hybrid carriers are aimed to enhance the stability, recovery and reusability of the enzyme used in the biocementation process. The results showed that the fabricated copper phosphate-based inorganic hybrid was stable throughout the duration of the tests (2 months) and under a wide range of pH and temperatures. Its enzymatic activity was enhanced compared to the free CA enzyme and it was proved suitable for soil biocementation. This was further confirmed by the SEM analysis. Additionally, the treated soil with the formulated hybrid carrier showed improved unconfined compressive strength, especially when the carriers were implemented into the soil by mixing. The material analysis by Raman spectroscopy confirmed calcium carbonate as the primary precipitate, consistent with soil biocementation. Overall, this innovative method of delivery of enzymes with enhanced stability and activity shows promise that, upon further development, it can be successfully used to increase the efficiency and sustainability of the biocementation process.

**Keywords:** carbonic anhydrase; enzyme carriers; ground improvement; biocementation; $CO_2$ capture



**Citation:** Mwandira, W.; Purchase, D.; Mavroulidou, M.; Gunn, M.J. Synthesis and Utilisation of Hybrid Metal-Carbonic Anhydrase Enzyme Carrier System for Soil Biocementation. *Appl. Sci.* **2023**, *13*, 9494. https://doi.org/10.3390/app13179494

Academic Editors: Paulo José da Venda Oliveira and António Alberto Santos Correia

Received: 6 July 2023
Revised: 12 August 2023
Accepted: 19 August 2023
Published: 22 August 2023



## 1. Introduction

Biocementation has recently emerged as a nature-inspired method of producing eco-friendly cement, with a reduced environmental impact and carbon footprint compared to Portland cement [1–4]. The process of biocementation uses organic and inorganic compounds to produce mechanically robust biomaterials [5]. Most biocementation studies use carbonates to biocement soils. The carbonates formed can store carbon permanently in the ground and potentially reduce the amount of $CO_2$ accumulation in the atmosphere [6]. Biocementation can be realised by different pathways, such as urea hydrolysis [7], denitrification [8], carbonic anhydrase [9] and methane oxidation [10] amongst others, or by a combination of processes [11].

The most common biocementation techniques to date are microbially induced calcium carbonate precipitation (MICP) or enzyme-induced calcium carbonate precipitation (EICP) [2,12,13]. MICP can have limitations for in situ applications in fine-grained soils, if precultured bacteria are injected in the soil to increase the bacteria population favourable for biocementation (bioaugmentation). This is because of the relatively large size of bacteria compared to that of the pore throats in fine-grained soils [14] (bacterial cells have cell sizes ranging usually from 0.5 to 3 μm). Additionally, living microorganisms are difficult to handle, as they are sensitive to environmental conditions [15,16]. EICP was therefore

proposed to overcome these problems associated with MICP. In EICP, free enzymes derived from microbes or plant sources have been suggested and used as a catalyst to produce biocement [2,17,18]. The use of free enzymes facilitates the injection of biocementation treatments in fine-grained soils with narrow pore-throat sizes and bypasses the complexity of controlling living organisms in situ. However, EICP also comes with limitations, as the use of free enzymes in soils entails different challenges. These are linked predominantly to: (a) the stability of the enzyme once released into the ground; (b) the limited enzyme supply (as there is no generation of more enzymes from the soil bacteria, unlike when microbial biocementation is used) and (c) the poor reusability of the enzyme, which increases treatment costs.

Previous studies for different applications have addressed these challenges by immobilizing the enzymes using suitable enzyme carriers. For example, enzyme carriers have been used in bioconcrete [19] or for $CO_2$ capture in bioreactors [20]. In $CO_2$ capture applications, hybrid enzyme–metal nanoflower carriers have been extensively used to achieve higher enzyme activity and stability [21]. The term "nanoflower" is used because the structure formed resembles a small flower.

The formation of enzyme–inorganic hybrid nanoflowers comprises a four-step mechanism, namely (a) the coordination, (b) coprecipitation, (c) self-assembly and (d) size growth of the hybrid nanoflower carriers [22]. The process was demonstrated in previous studies, where metal ions were shown to react with phosphate ions to form the first crystals. Once the crystal is created, the metal ion complexes with the enzyme, producing a "nanoflower". Previous studies have shown that the formation process of nanoflower enzyme carriers by encapsulation, adsorption and covalent attachment to flower-like structures is efficient and that the carriers are stable [23–26].

Because of these advantages, the present study combined an inorganic metal ion and carbonic anhydrase (CA) enzyme to fabricate a stable enzyme carrier based on the hybrid enzyme–metal nanoflower method. The study is a proof-of-concept of the hybrid nanoflower technique for soil biocementation using the CA pathway, for concurrent $CO_2$ absorption and soil stabilisation.

The CA biocementation pathway adopted in this study is proposed as an innovative, eco-friendly, sustainable soil stabilisation method that can consume $CO_2$ from the atmosphere or use captured $CO_2$ to precipitate $CaCO_3$, which binds together (i.e., biocements) soil particles. In this multi-step chemical process, CA catalyses the precipitation of calcite. The aqueous $CO_2$ (aq) formed (Equation (1)) reacts with water to form $H_2CO_3$ (Equation (2)). The absorption of $CO_2$ in an aqueous medium entails the conversion of $CO_2$ (aqueous) to $HCO_3$ (Equation (3)). CA enzyme can substantially increase the rate of $CO_2$ mineralization by CA-catalysed hydration of $CO_2$ to $HCO_3$. This $CO_2$ -derived $HCO_3$ can be mineralized to metal carbonates that can be stored as $CO_2$ minerals or used in value-added chemicals and other products/materials (adhesives, sealants, food additives, pharmaceuticals, paints, coatings, paper, cement and construction materials [26]).

$$CO_2\ (g) \leftrightarrow CO_2\ (aq) \quad (1)$$

$$CO_2\ (aq) + H_2O\ (l) \leftrightarrow H_2CO_3\ (aq) \quad (2)$$

To form a biocement via biomineral precipitates, the metal ion, e.g., $Ca^{2+}$, reacts with $CO_3^{2-}$ (Equation (5)), forming calcium carbonate, where the CA enzyme provides nucleation sites.

$$H_2CO_3(aq) \leftrightarrow H^+ + HCO_3^-\ (aq) \quad (3)$$

$$HCO_3^- \leftrightarrow H^+ + CO_3^{2-} \quad (4)$$

$$Ca^{2+} + CO_3^{2-} \leftrightarrow CaCO_3\ (s) \downarrow \quad (5)$$

Due to the simplicity of the process, CA-mediated mineralization has become one of the most popular ways of $CO_2$ conversion and utilization. There are many examples in the literature, demonstrating that stabilized and immobilized CA drastically enhances $CO_2$ mineralization and retains most of its $CO_2$ mineralization capacity after many cycles of $CaCO_3$ mineralization for faster and more efficient $CO_2$ conversion and utilization (see, e.g., [26,27]). Thus, a major industrial application of hybrid delivery systems is for carbon capture and storage (CCS) and carbon conversion and utilisation (CCU) technologies, where a basic requirement for the success of the processes is the adequate transfer of $CO_2$ from the gas phase to the aqueous phase. This critical requirement can be addressed by the use of the CA enzyme, whose active site contains hydroxide-bound $Zn^{2+}$ for catalysis of the interconversion between $CO_2$ and bicarbonate. However, a major challenge for the industrial implementation of CA is the poor stability of CA at high temperatures, in alkaline pH, or in the presence of high salt concentrations. Thus, producing robust CAs is essential; CA immobilization in hybrid nano-carriers is one way of addressing this challenge, while also enabling the easier recovery and reuse of enzymes, lowering the cost of CA per ton of captured/utilized $CO_2$. Furthermore, immobilization and stabilization of CA in nanostructured materials, allows CA to be placed together closely with other $CO_2$-converting enzymes; this way $CO_2$ captured by CA can be transferred to other enzymes in order to improve the kinetics of $CO_2$ conversion. CA immobilization and stabilization in nanostructured materials also allows for the combination of immobilized CA with $CO_2$-converting microorganisms. Overall, the immobilization of CA with nanostructured carriers gives promise for the development of highly stable and reusable CA for the faster and more efficient $CO_2$ conversion and utilization [28].

Inspired by the literature covering CCC and CCU, this paper aims to assess, for the first time, the feasibility of using immobilized CA in hybrid carriers, as an efficient enzyme delivery system for soil biocementation applications by EICP. The supply of the enzyme through the hybrid carrier aims to overcome challenges of the EICP biocementation method linked to enzymatic stability and supply issues. This would be a useful advancement in improving the EICP technique, while also proposing a method of mineralizing $CO_2$ in the process, which could create a carbon sink. Also, in view of the proposed electrokinetic implementation of the treatments by the authors to address treatment delivery under existing infrastructure [29], it seems practical to use the same electrokinetic system in situ for the recovery of the hybrid carriers for future reuse.

The particular novelty of our experimental (laboratory) research is therefore the synthesis and study of the performance of a stable metal–organic hybrid enzyme carrier aimed for biocementation applications in soil stabilization; this is investigated for the first time. The research is unique and different from previous studies on hybrid nanoflower carriers, which did not consider soil biocementation applications. It is also innovative compared to other biocementation studies as: (a) it proposes the novel enzyme delivery system for biocementation applications; (b) it aims to produce biocement to stabilize soils while capturing $CO_2$ at the same time, thus contributing to the net-zero targets of the construction industry; this is unlike most other biocementation studies, based on the ureolytic route.

The following sections present the synthesis and utilisation of a metal–organic hybrid carrier based on the principle of nanoflower synthesis for the delivery and stabilisation of CA enzymes with enhanced enzymatic activity.

## 2. Materials and Methods

### 2.1. Materials Used

The soil used in this study was a sandy silty clay sampled from the Prickwillow site of the East Anglia railway network (East Cambridgeshire, Eastern England X/Y co-ordinates: 559,276, 282,290). Soil samples from the railway embankment were obtained by rotary drilling method. Undisturbed soil samples were collected using tube samplers. Figure 1 shows the particle size distribution of the soil from 1.2 to 2.2 m depth, which was used in this study. Table 1 shows some basic physicochemical characteristics of the soil.

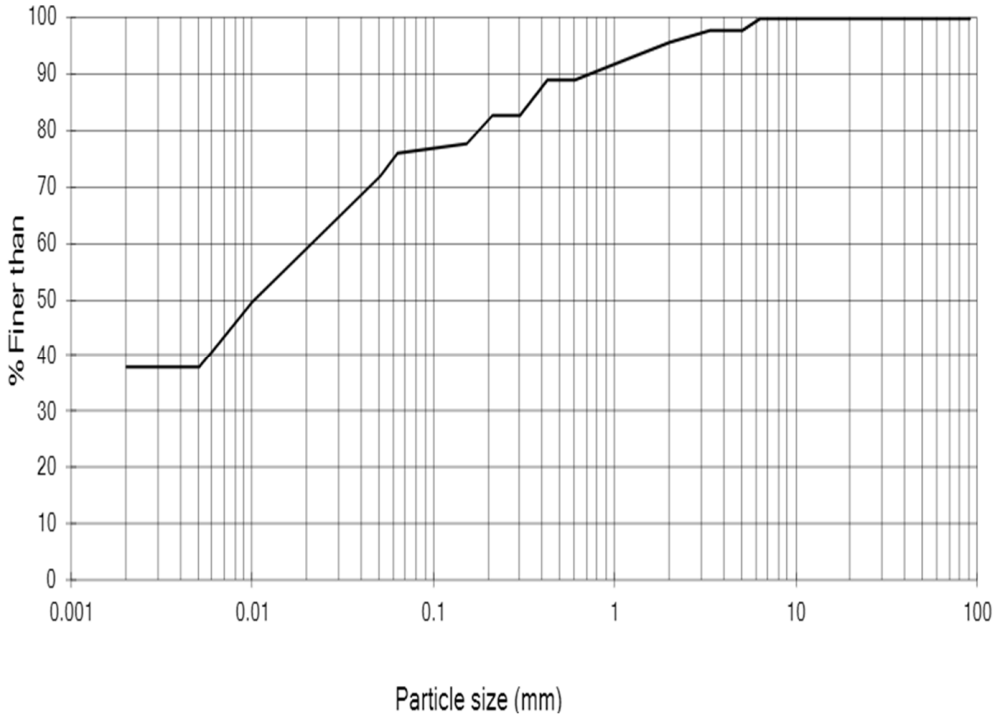


**Figure 1.** Particle size distribution of the soil used in this study.

**Table 1.** Basic physicochemical properties of a sandy silty clay soil from Prickwillow, East Anglia.

| Property | Value | Test/Standard |
|---|---|---|
| Liquid limit: % *w*/*w* | 63 | Cone penetrometer; BS 1377-2: 1990 [30] |
| Plastic limit: % *w*/*w* | 33 | BS 1377-2: 1990 [30] |
| Plasticity index: % *w*/*w* | 30 | BS 1377-2: 1990 [30] |
| Gravel content (%) | 4 | BS 1377-2: 1990 [30] |
| Sand content (%) | 20 | BS 1377-2: 1990 [30] |
| Silt content (%) | 37 | BS 1377-2: 1990 [30] |
| Clay content (%) | 39 | BS 1377-2: 1990 [30] |
| Soil classification | CH | BS 1377-2: 1990 [30] |
| Organic matter content: % *w*/*w* | 3.9 | Loss of ignition: ASTM D2974-14 [31] |
| Moisture content: % *w*/*w* | 47.5 | BS EN ISO 17892: Part 1: 2014 [32] |
| In situ bulk density (g/cm$^3$) | 1.78 | BS EN ISO 17892: Part 2: 2014 [33] |
| pH | 7.7 | BS ISO 10390:2005 [34] |
| Natural $CaCO_3$ content (%) | 4.82 | ASTM D4373-21 [35] |
| Undrained shear strength, $S_u$ (kPa) | 5.5 | Unconfined compression test BS EN ISO 17892-7:2018 [36] |

For the synthesis of the enzyme carrier, copper sulphate, manganese sulphate, cobalt sulphate, titanium sulphate, calcium chloride, sodium bicarbonate, 4-nitrophenyl acetate (p-NPA) and carbonic anhydrase (CA) from bovine erythrocytes (E.C.4.2.1.1) were obtained from Sigma-Aldrich. Ultra-pure water was used to formulate stock solutions of these salts.

### *2.2. Synthesis of Metal–CA and Measurement of CA Activity*

The metal–CA hybrid carrier assay was synthesised according to the Duan research group's protocol, which produced hybrid nanoflower carriers for $CO_2$ capture [25]. Briefly, the procedure used was the following: 0.6 mL of metal phosphate solution (Ti, Co, Mn, Cu, Ca and Zn) of 120 mM was added into 100 mL of phosphate-buffered saline (PBS, 0.1 M, pH 7.4) solution containing 10 mg of CA and was incubated at 4 °C for 2.5 days, as illustrated in Figure 2. The red and blue dots in Figure 2 represent phosphate and metal ions, respectively, in the reaction. The activity of the CA enzyme was determined spectrophotometrically by mixing p-nitrophenyl acetate (p-NpA) hydrolysis at room temperature in

a reaction mixture (1.35 mL) containing freshly prepared 3 mM p-nitrophenyl acetate in phosphate buffer (0.13 M and pH 7.2). Activity for p-NpA hydrolysis was determined using a method that Armstrong and the group proposed in 1966 [37]. The reaction proceeded for 5 min, and the change to $A_{348}$ per minute was measured. Then, the CA activity was characterised by the amount of p-nitrophenol produced per unit of time, and enzyme activity was expressed in terms of U (see Equation (6)):

$$\text{CA activity}\left(\frac{\text{U}}{\text{mL}}\right) = \frac{(A_{348}\text{T} - A_{348}\text{B}) \times 1000}{5 \times Volume} \quad (6)$$

where $A_{348}$T is the final reading of absorbance; $A_{348}$B is the initial uncatalysed reaction at a wavelength of 348 nm; and 1 U (μmol/min) is defined as the amount of the enzyme that catalyses the conversion of one micromole of substrate per minute.

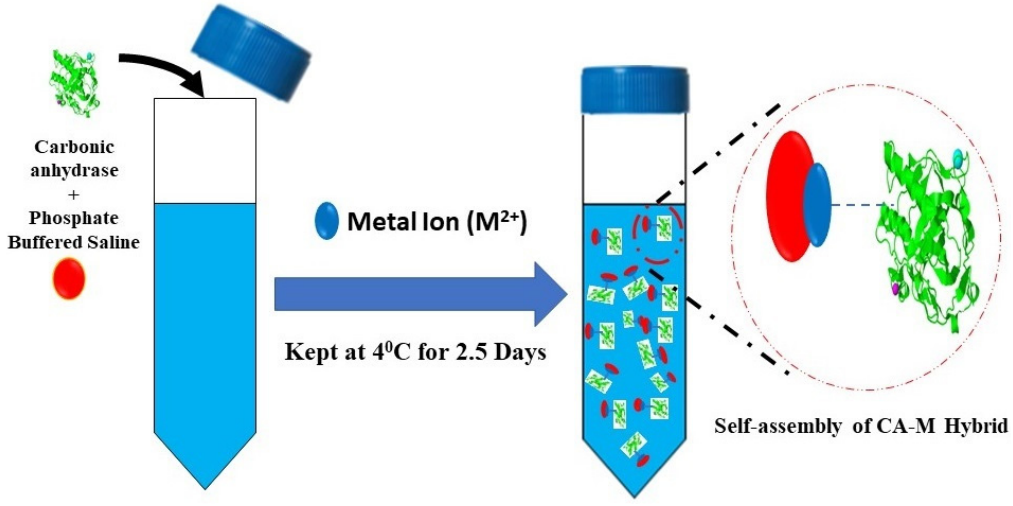


**Figure 2.** Schematic representation of nanoflower of CA–metal synthesis.

### *2.3. Effect of pH and Temperature on the Stability of CA and CA-Cu*

The activity of the CA and CA-Cu was determined at various reaction pH ranges and temperatures. For the thermal stability investigation, the temperature in the incubator shaker was maintained at 5, 10, 15, 25, 37, 50 and 60 °C under the constant pH of the PBS buffer (pH = 7.4), whereas the study of the stability of the enzyme at different pH values (pH 7, 8, 9, 10 and 11) was performed at room temperature.

### *2.4. Bioprecipitation Testing and $CO_2$ Capture Ability*

Bioprecipitation experiments in a total volume of 30 mL were conducted using cementation solution (i.e., sodium bicarbonate ($NaHCO_3$) and calcium chloride ($CaCl_2$)) with either free CA or Cu-CA hybrid carriers. Water was used as the control medium. The composition of each system is shown in Table 2. Each bioprecipitation experiment was conducted in a conical flask at 25 °C, 120 rpm, and the investigation lasted for 24 h. Precipitation experiments were conducted in triplicate.

### *2.5. Characterisation Analysis*

#### 2.5.1. Aqueous Chemistry Measurements

The pH and conductivity of each system were monitored using a Hanna Instruments (Bedfordshire, UK) HI 9813-6N Waterproof pH/EC/TDS Temperature Meter. The total amount of bioprecipitate formed in each system was measured by discarding the supernatant after centrifuging, and the biomineral was dried and weighed.

**Table 2.** Experimental conditions for bioprecipitation and $CO_2$ capture ability.

| | Water (mL) | CA (mL) | CA-Cu (mL) | $CaCl_2$ (mL) | $NaHCO_3$ (mL) |
|---|---|---|---|---|---|
| **Bioprecipitation** | | | | | |
| Control | 10 | 0 | 0 | 10 | 10 |
| Free CA enzyme | 0 | 10 | 0 | 10 | 10 |
| Cu-CA hybrid carrier | 0 | 0 | 10 | 10 | 10 |
| **$CO_2$ capture ability** | | | | | |
| Control | 100 | 0 | 0 | 100 | 0 |
| Free CA enzyme | 0 | 100 | 0 | 100 | 0 |
| Cu-CA hybrid carrier | 0 | 0 | 100 | 100 | 0 |

#### 2.5.2. SEM and Raman Analysis

The microstructure of the biomineral formed was analysed using scanning electron microscopy (SEM) with Thermo Scientific Pharos FEG-SEM (ThermoFisher Scientific, Waltham, MA, USA) with high vacuum mode, 15 KV acceleration voltage; elemental analysis was performed with an energy dispersive X-ray detector (EDS). Raman spectroscopy (LabRAM ARAMIS confocal Raman microscope Horiba Jobin-Yvon, Villeneuve d'Ascq, France) with 633 nm laser (1% power), 50X objective, 100 µm pinhole, 600 L/mm grating was used.

#### 2.5.3. Calcium Carbonate Content Measurement

The $CaCO_3$ content was determined using the acid-washing technique. This technique measured the oven-dried mass at 105 °C before and after an acid wash in a 2 M solution of HCl. The difference between the two masses was taken as the calcium carbonate mass.

### *2.6. Biocementation Experiments Design*

The biocementation treatments were implemented in the soil using two different methods: injection and mixing. The injection was executed in two stages: in the first stage, the synthesised hybrid enzyme carrier was injected into cylindrical soil specimens of 50-mm diameter and 100-mm length; then, the cementation solution of $CaCl_2$ and $NaHCO_3$ (0.1 M) with a pH = 8.5 was injected at the top of the soil specimens at a rate of 3 mL/min and was allowed to percolate by gravity. For the mixing method, the treatments were implemented by hand mixing for 3 min using different mixing ratios of $CaCl_2$, $NaHCO_3$ and water, CA and CA-Cu hybrid enzyme carrier, as shown in Table 3. The molarity of the cementation solution used was based on prior optimisation conducted for bioprecipitation. A set of control specimens (untreated soil) was also prepared for comparison purposes, as shown in Table 3. The unconfined compressive strength testing (UCS) of the 50 mm diameter and 100 mm length soil specimens was measured using a Multiplex 50–48-kN loading frame. The axial load was applied at a constant rate of 1%/min.

**Table 3.** Experimental conditions for biocementation treatment by injection and mixing.

| Treatment Option | Description | Sandy Silty Clay Soil(g) | $CaCl_2/NaHCO_3$ (M) | Sterile Distilled Water (mL) | CA Enzyme (mL) | CA-Cu Enzyme (mL) | Curing Time (Day) |
|---|---|---|---|---|---|---|---|
| Injection | Control | 300 | 0.0/0.1/0.2/0.5 | 1.5 P.V | 0 | 0 | 7 |
| | CA Only | 300 | 0.0/0.1/0.2/0.5 | 0 | 1.5 P.V | | 7 |
| | CA-Cu | 300 | 0.0/0.1/0.2/0.5 | 0 | 0 | 1.5 P.V | 7 |
| Mixing | Control | 300 | 0.0/0.1/0.2/0.5 | 50 | 0 | 0 | 7 |
| | CA Only | 300 | 0.0/0.1/0.2/0.5 | 0 | 50 | 0 | 7 |
| | CA-Cu | 300 | 0.0/0.1/0.2/0.5 | 0 | 0 | 50 | 7 |

All experiments were performed in triplicate ($n = 3$) to reduce the experimental errors and confirm the variability and validity of the results.

## 3. Results and Discussion

### *3.1. Synthesis of Hybrid Enzyme–Metal Carriers*

The synthesis results of hybrid enzyme–metal carriers are shown in Figure 3a–f for the different morphologies of the metal tested, including Ti, Co, Mn, Cu, Ca and Zn. Based on the morphology of the carriers (which were flower-shaped), these will be referred to as 'nanoflowers' for simplicity, as in previous investigations [38,39]. However, in this study, the sizes of the carriers were of the order of several microns. As observed from the SEM images, only the copper nanoflowers were successfully formed; the other metal ions tested failed to produce flower-shaped hybrid carriers [21]. The shape of nanoflowers is essential as it contributes to the high surface-to-volume ratio of the flowers, thus enhancing surface adsorption for accelerating the kinetics of reactions [40]. Despite changing the pH, metal concentration, and enzyme concentration, no flower-shaped carriers were observed when using other metal ions. Several previous studies have also alluded to the failure to develop nanoflowers and have concluded that the formation of nanoflowers is sensitive to experimental conditions [40–42]. It could therefore be postulated that the optimal conditions for nanoflower formation were not met. This could probably be due to two critical factors in nanoflower synthesis: medium environment [43] and surface chemistry of the enzyme biomolecules [44]. As reported, these two parameters are essential for the organic–inorganic hybrid nucleation, growth and assembly. Thus, the results in the following sections and discussion are based on only the copper hybrid carrier (CA-Cu), whose morphology shown in Figure 3d was similar to that reported by previous studies [21,25].

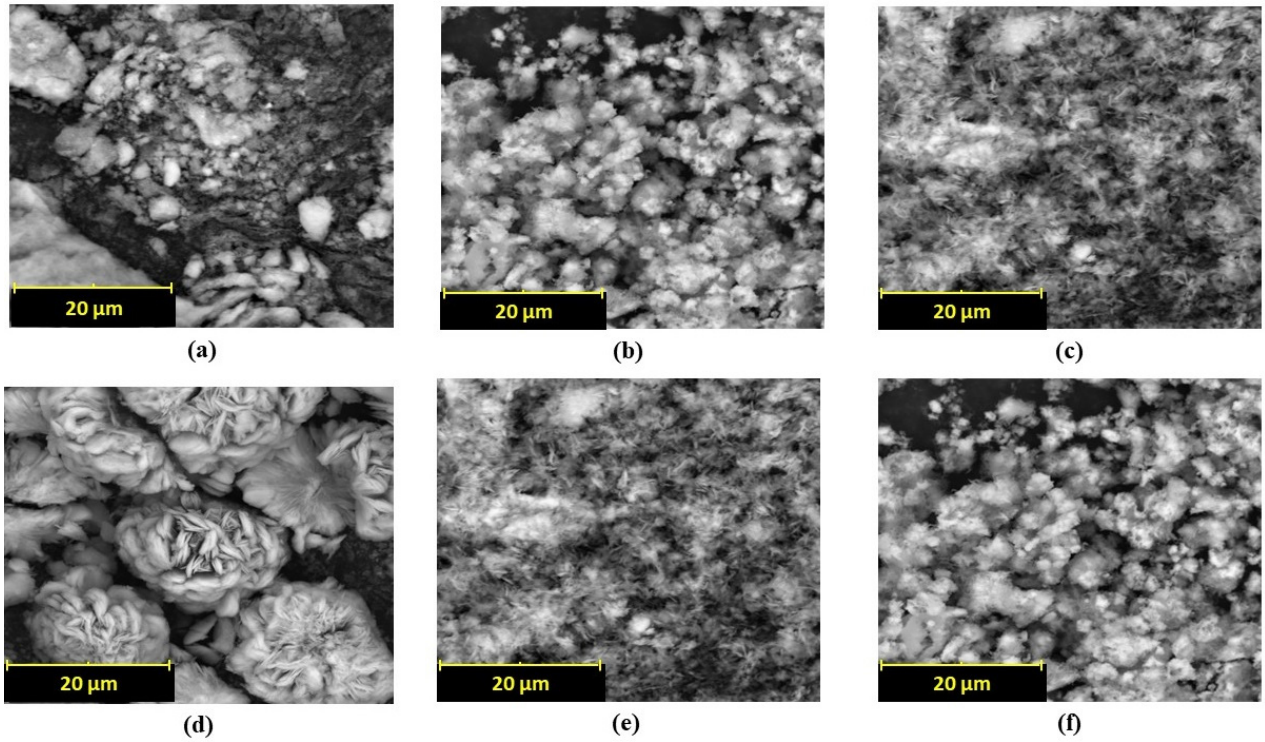


**Figure 3.** SEM images of (**a**)Ti-CA hybrid carriers, (**b**) Co-CA hybrid carriers, (**c**) Mn-CA hybrid carriers, (**d**) Cu-hybrid carriers, (**e**) Ca-CA hybrid carriers, (**f**) Zn–CA hybrid carriers.

Figure 4a–d shows the flower-like structures for the Cu-CA hybrid, confirmed by SEM images. These showed good dispersity of the petals with three-dimensional microstructures. Specifically, the hybrid "nanoflowers" presented a unified structural morphology like a "Dahlia pinnata", as depicted in the final image of Figure 4d. Since the inceptive

investigations of new nanomaterials in the mid-2000s, different organic–inorganic nanomaterials have been created with different metal ions and organic components exhibiting different morphologies [45]. Previous studies have confirmed that nanoflower morphology is affected by the concentration of reactants and solvent conditions. Thus, there is a plethora of different nanoflower morphologies as can be attested in the literature [23,40]. Different morphologies of each type of nanoflower have different applications, discussed in the Introduction and Discussion sections.

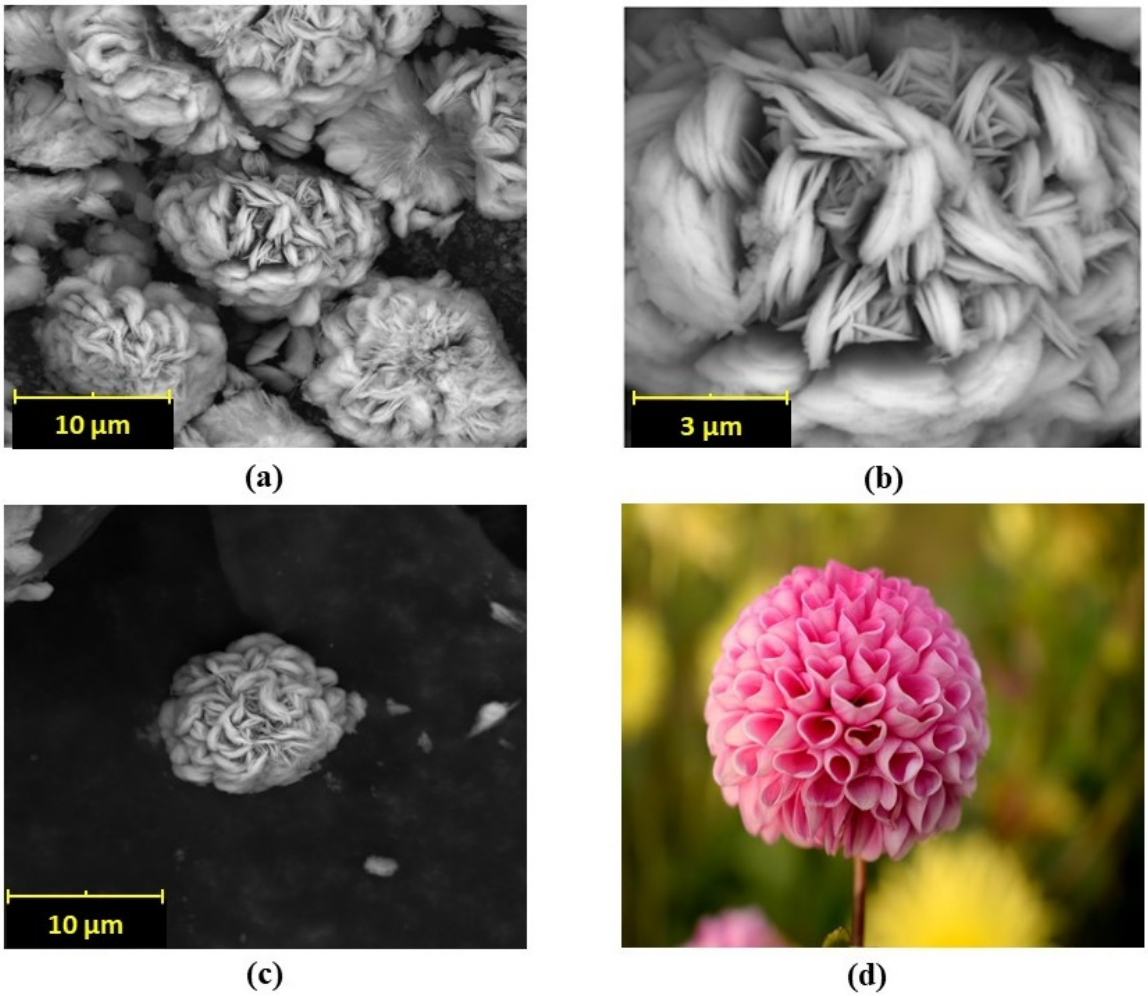


**Figure 4.** (**a**–**c**) SEM images of Cu-CA hybrid nanoflower at different magnifications (coloured photograph courtesy of public resources in the network), (**d**) a "Dahlia pinnata" flower.

### *3.2. Stability of CA-Cu and $CO_2$ Capture Ability*

We compared the relative activity of both the free and immobilised enzyme. The relative enzyme activity is the ratio of the retained activity of an immobilised CA or a free enzyme and was investigated over 60 days. The results in Figure 5 showed that the immobilised enzyme efficiency was 95%. Previous studies presented similar findings for the immobilised CA [46,47]. In our study, the free CA enzyme lost 34% of its initial activity within 7 days when incubated in PBS (pH 7.4) at room temperature. Conversely, CA-Cu hybrid carriers maintained 94% of their initial activity under the same conditions even after one month (Figure 5a). Thus, the immobilisation strategy lowers enzyme deactivation so that enzymes can be used for extended periods, as previously reported [48]. The increased stability of the CA-Cu is crucial as it is an essential factor in biocementation.

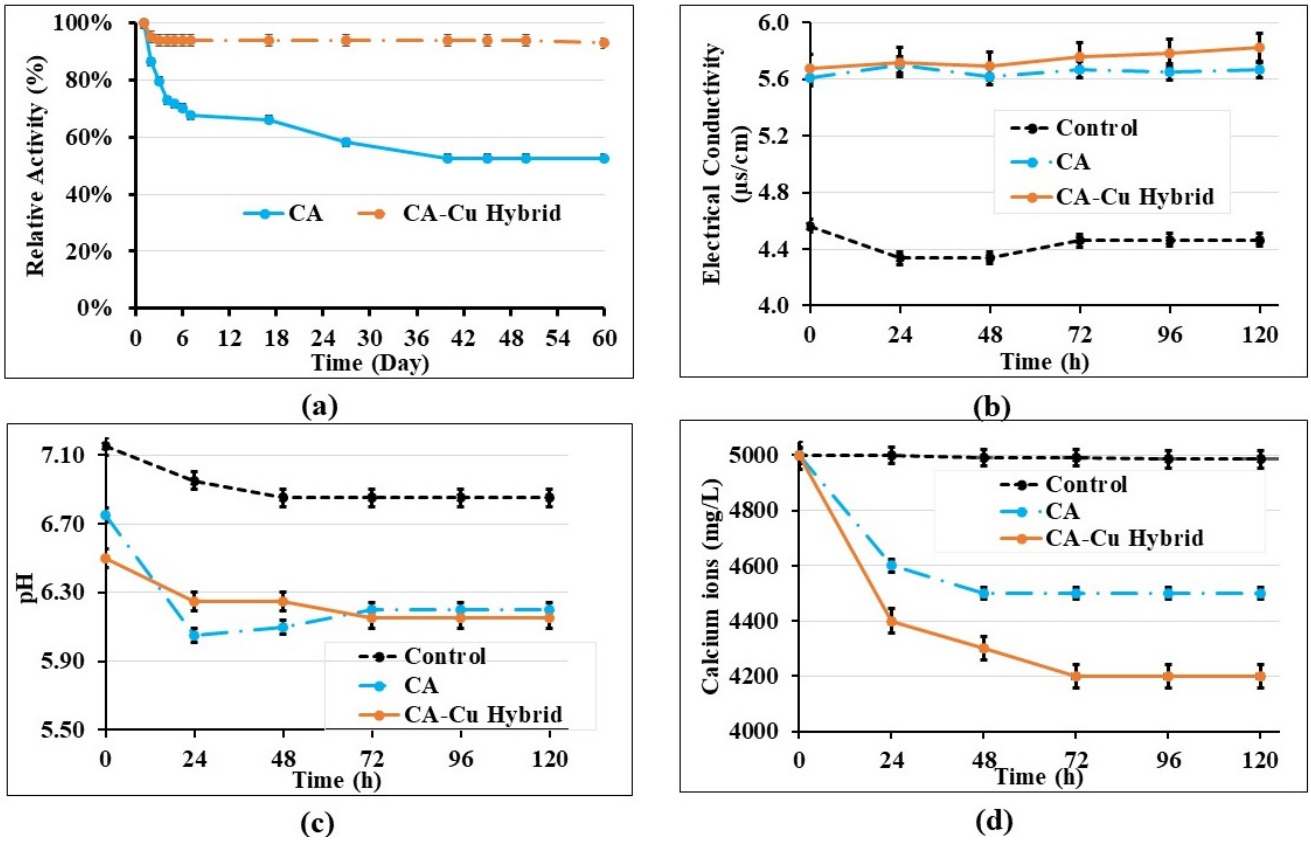


**Figure 5.** (**a**) Stability of CA and CA-Cu hybrid over time, (**b**) electrical conductivity changes over time, (**c**) pH changes over time, (**d**) change curve of calcium concentration.

The pH stability of the free CA and immobilized CA-Cu was assessed after incubating at specified pH values. pH is a critical factor in biocementation, as it controls the precipitation and dissolution of biominerals; the enzyme is therefore required to be stable in the alkaline range where calcite bioprecipitation occurs [19]. Figure 6a shows the relative activity of the CA enzyme (free or immobilized) compared to the initial activity of the enzyme, under different pH values. From Figure 6a, it can be seen that when the incubation pH increased, the free enzyme lost its activity steadily but still preserved about 85% of its stability at pH > 9. On the other hand, the immobilized CA was even more stable retaining about 92% of its original activity at pH > 9. Similar results from the literature also showed that the CA enzyme remained stable and maintained its secondary structure for pH values of 7.0–11.5 [49].

The activity of the free and immobilised CA enzyme was also measured under different temperatures; the results are presented in Figure 6b in terms of the relative activity of the enzyme compared to its initial activity. The free enzyme lost approximately 30% of its activity at temperatures higher than 50 °C. The activity loss of the CA-Cu at the same temperature range was only 10%. Overall, the activity of the immobilized CA was minimally affected for a wide temperature range until around 40 °C, when a more notable activity loss started. Previous studies also found that immobilised CA enzyme had a higher thermal stability/activity than the free CA enzyme and that the optimal temperature for CA immobilized within polyurethane foam was 40 °C [50]. Other studies of thermostable CA found it to be active in the temperature range 0–100 °C, with an optimal temperature of approximately 80 °C [51]. Despite the difference in optimal temperature observed in the two papers, it can be concluded that CA enzymes can operate at wide temperature ranges. This finding is important, as in biocementation it is critical that the enzyme remains stable at different soil temperatures. In our study, we investigated temperature ranges from 5 to 60 °C; we found the immobilised enzyme to lose only up to 10% of its initial

activity within this temperature range; moreover, only a 1–2% activity loss was observed for temperatures up to 35 °C. The foundation soil temperature commonly ranges between 10 and 24 °C. Therefore, the CA and CA-Cu enzymes would suit ground improvement applications in most world regions, while contributing to climate change mitigation by converting $CO_2$ into calcium carbonate. Comparing the proposed method to using bacteria for biocementation, cultivation of the latter could be challenging if in situ temperatures and pH were unsuitable for bacterial growth and survival.

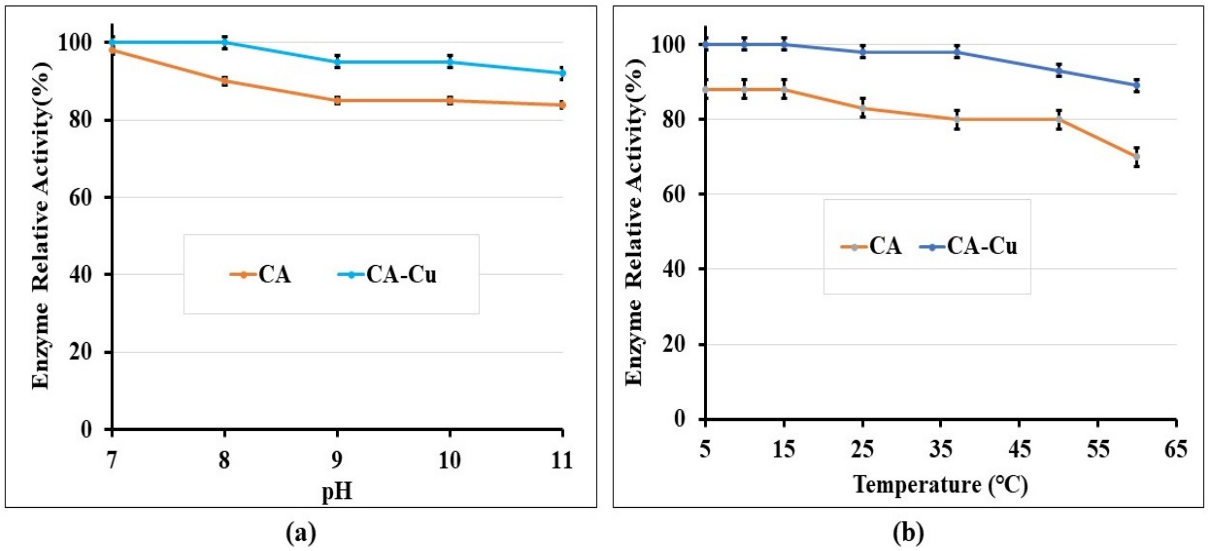


**Figure 6.** (**a**) Stability of CA and CA-Cu hybrid under different pH; (**b**) Stability of CA and CA-Cu hybrid under different temperatures.

To understand the $CO_2$ capture of the synthesised CA-Cu and free CA, the water chemistry was investigated, and the pH (Figure 5b), electrical conductivity (Figure 5c) and calcium ion content (Figure 5d) were determined. As shown in Figure 5b, CA-Cu and free CA systems showed an increased electrical conductivity compared to the water-only system. This difference in electrical conductivity is due to the $CO_2$-$H_2O$ system, whereupon $CO_2$ dissolution in the water, there is the formation of $HCO_3^-$ leading to increased conductivity. In the control samples with water only, the electrical conductivity and pH remained relatively the same, as in the water-only system, the dissolution of $CO_2$ in water was limited. Consistently with what was previously reported, the results of the present study showed that immobilised CA is more stable over time and contributes to $CO_2$ capture and precipitation [40,52]. Bioprecipitation is confirmed by the reduction in calcium ion content as the CA captures $CO_2$ from the atmosphere and forms biominerals. Conversely, the water-only system did not show any changes in calcium concentration (Figure 5d) as no precipitate was observed.

Enzyme immobilisation has been used in industrial biotechnology to reduce costs [20,53]. Thus, this study postulated that the proposed method would reduce the costs of biocementation, as the immobilisation process is inexpensive and could allow large amounts of recoverable and reusable enzyme to be prepared for large-scale biocementation. Although, arguably, the hybrid carrier synthesis would incur some extra costs compared to the use of free enzymes, in the longer term, the savings coming from the reuse of the hybrid carriers (which are recoverable and can maintain their activity at various temperatures and pH conditions for a long time) would outweigh the synthesis costs.

### *3.3. Bioprecipitation in Liquid Batches*

A bioprecipitation experiment in liquid batches was conducted to attest calcite formation using the synthesised CA-Cu nanoflower with a calcium source. The bioprecipitation results showed the distinct difference in morphology between precipitates from chemical

reactions without enzyme and enzyme-promoted bioprecipitation, as shown in Figure 7a–c. The chemical reaction between $CaCl_2$ and $NaHCO_3$ without enzymes showed a combination of spherical and cubic morphology of calcite at different equimolar concentrations. However, different morphologies were seen in both free CA and CA-Cu nanoflower bioprecipitation. Generally, the reaction proceeds slowly at low equimolar concentrations forming mainly amorphous and irregular unidentifiable crystals seen in either the CA or the CA-Cu nanoflower case. The difference is, however, that the CA-Cu nanoflower had nanoflower co-precipitate together with the calcite, as seen in Figure 7c. Calcite is the most stable form of calcium carbonate compared to vaterite and aragonite. The findings are consistent with the study by Li et al. on the calcium carbonate induced by carbonic anhydrase, which also revealed calcite formation after 24 h of bioprecipitation [54].

The results from Raman's spectroscopy identified the precipitates as calcite (Figure 8) (see the matching signals of the three superimposed spectra in Figure 8, which include those of calcite mineral). The peaks corresponded to the lattice vibration of calcite and the in-plane bending vibration peak of the carbonate group of calcites at approximately 716 $cm^{-1}$ and were therefore identified as calcite. For Raman spectroscopy, the peak at 288 $cm^{-1}$ arises from the vibrations of the $CO_3^{2-}$ groups that involve rotatory oscillations of those groups. The results thus indicate that both the free CA and the Cu-CA carrier enzymes can be used to biocement soil due to calcite production, as previously reported [55]. This result suggests that Cu-CA hybrid carriers can be a good alternative to the free-enzyme catalysing calcite precipitation for soil biocementation.

### *3.4. Biocementation of Fine-Grained Soil Using CA-Cu Nanoflower*

#### 3.4.1. Unconfined Compressive Strength

Figures 9 and 10 show the fine-grained soil specimens after treatment with cementation solution, free CA and CA-Cu using injection and mixing, respectively. Table 4 summarises the results of each case for the control, CA and CA-Cu. According to the results, the maximum UCS of the biocemented soil increased by 85% for CA only, whereas for CA-Cu hybrid carrier mixed in the soil it increased by 319% compared to the control. On the other hand, the injection method showed a 116% increase for CA only and only a 38% increase for the CA-Cu nanoflower. Although this study aimed to use injection as a preferred method for nanoflowers, the results indicate the difficulty in injecting the CA-Cu into the fine-grained soil due to the size of the hybrid carrier, compared to the narrow pore throats in the soil matrix. This is reflected in the lower UCS values achieved and is confirmed by the non-uniform calcite precipitation in the specimen discussed later. Another possible reason for the observed UCS values upon injection is the rapid reaction of the CA enzyme involved in bioprecipitation. As shown in Figure 5d, the bioprecipitation process occurs spontaneously due to the action of the CA enzyme and the reaction is completed quickly. The rapid reaction naturally caused bioclogging of the top surfaces of the soil column, restricting the movement of both enzymes and the cementation solution. This severe bioclogging was observed in all CA-Cu cases; hence, the lower UCS values of the specimens treated by injection in Figure 9, as the treatments appear to have biocemented only the top surfaces of the soil specimens. Namely, in Figure 9, a thin layer of crust is seen to have formed on the top of all treated soil specimens (whether the treatment was caused by chemical reaction without enzymes (Figure 9a), chemical reaction with CA enzymes (Figure 9b) or CA-Cu carriers (Figure 9c) and for all solution molarities used); this crust was identified as calcium carbonate (see Figure 8). This biocement crust reduces the soil permeability on the top of the soil specimen by clogging the soil pores; it thus prevents the ingress of further treatments. Similar results have been frequently reported in previous studies for both the EICP and MICP processes. These studies have also shown the formation of a water-impermeable and high-strength crust layer on the soil surface (usually sandy soils) rather than a more uniform biocementation of the soil at further depth [56–59].

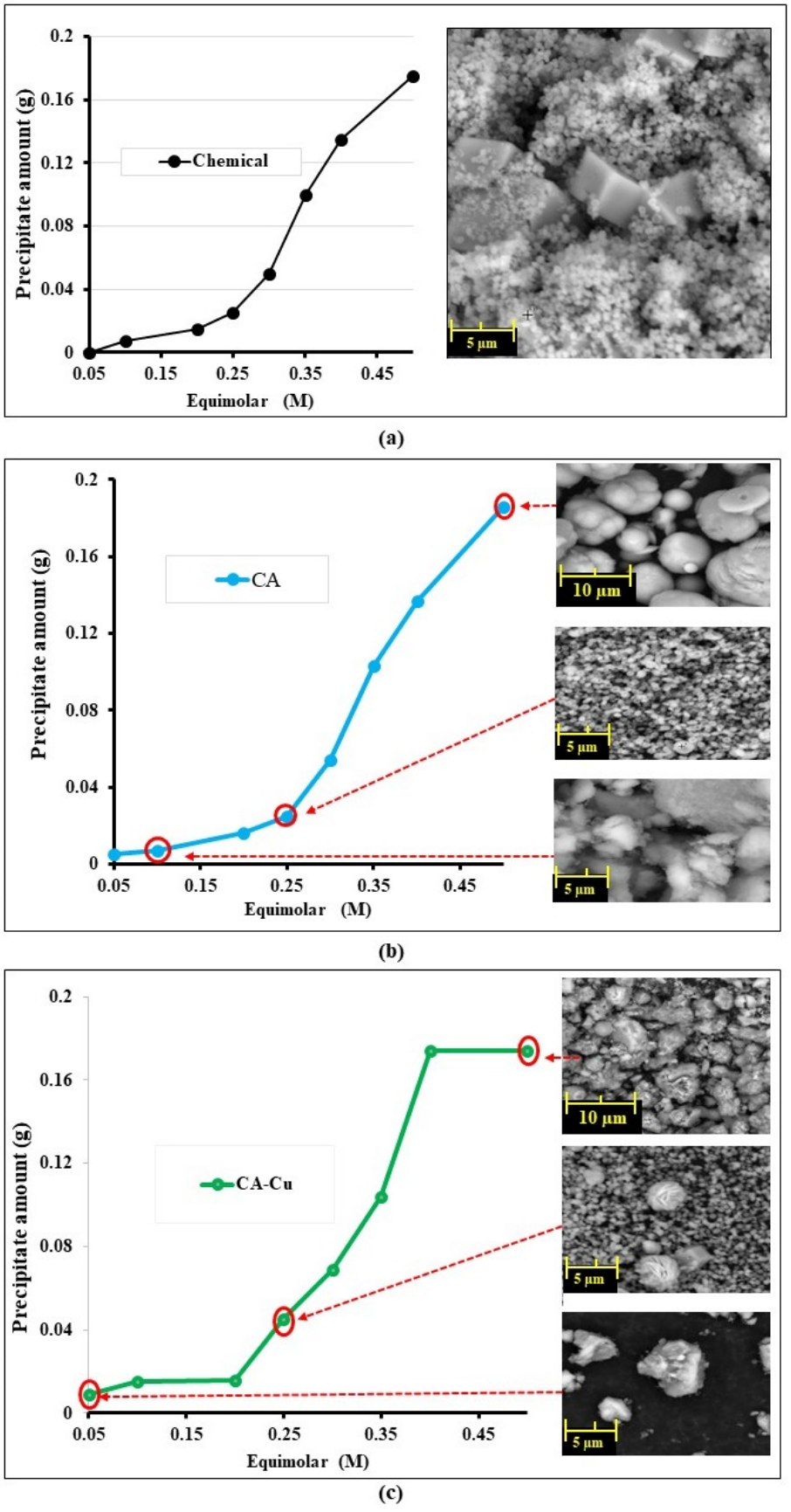


**Figure 7.** Bioprecipitation at different equimolar concentrations of $CaCl_2$ and $NaHCO_3$ (**a**) chemical reaction without enzyme, (**b**) carbonic anhydrase (CA) enzyme only, (**c**) CA-Copper nanoflower.

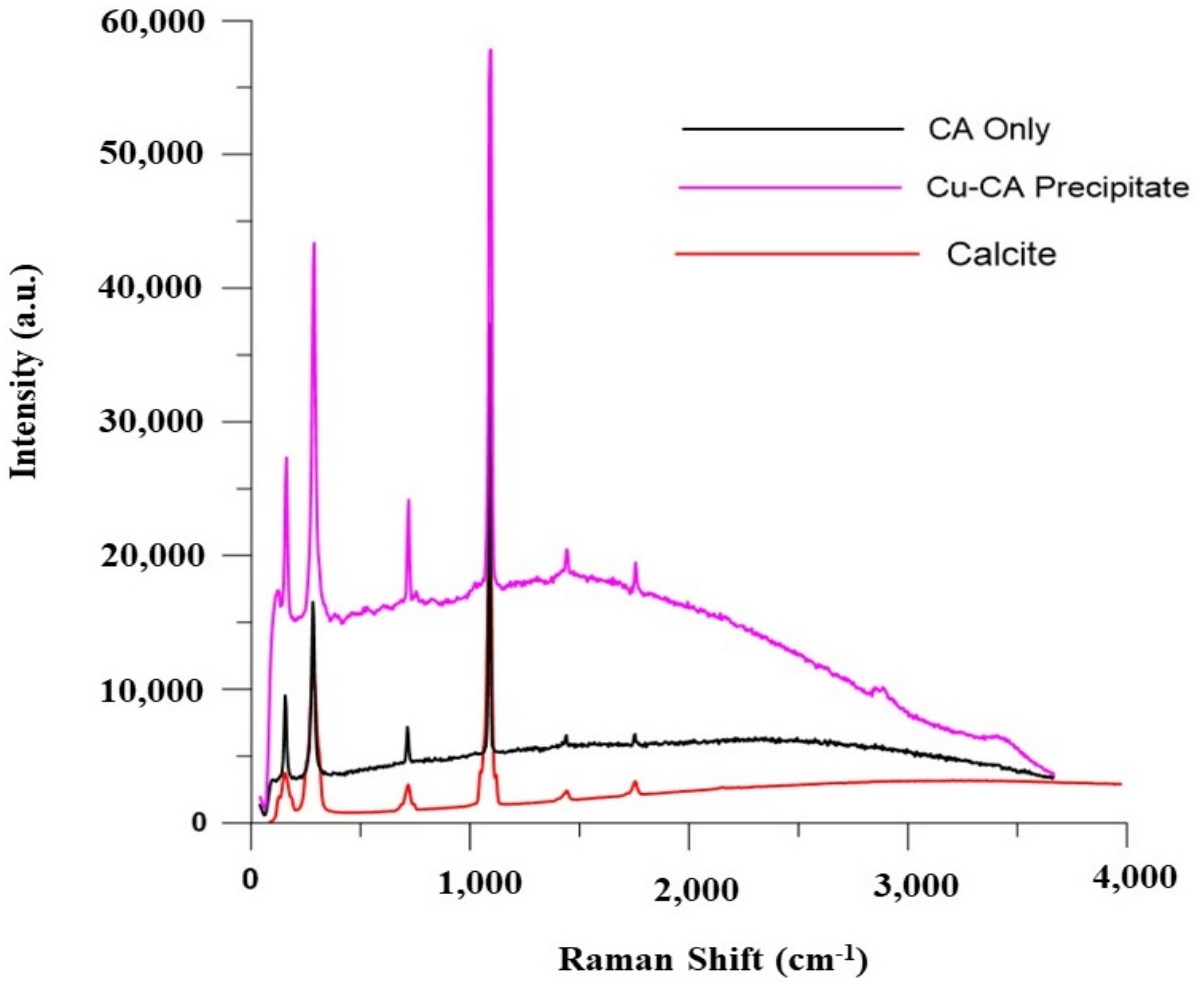


**Figure 8.** Raman spectroscopy of CA and CA-Cu hybrid carrier bioprecipitate (a.u. stands for 'arbitrary units').

Comparatively, the mixing method (Figure 10) was superior to the injection method (Figure 9), according to the results of this study. This was evidenced (a) by the higher strengths achieved as reported earlier; (b) by the absence of a localized biocement crust on the surface (as opposed to the injection method); (c) by an observed more uniform soft-rock-like consistency throughout the soil sample. Generally, the results showed that the synthesized CA-Cu enzyme was highly effective in biocementing the soil. Specifically, the CA-Cu carriers yielded over 300% increase in UCS compared to the control, when treatments were implemented by mixing; conversely, with the injection method a 38% increase was obtained using CA-Cu carriers. Mixing was therefore still the best way of treating fine-grained soil investigated in this study and this is consistent with the literature [38,39]. As shown in Figure 1, the investigated soil consisted of 39% clay. This is why it was difficult to treat the specimens by injecting enzyme carriers of a size of several microns. Thus, unless the size of the hybrid carrier is reduced and the injection sequence optimized, mixing would be the preferred method of implementation, if the desired outcome is a uniform biocementation throughout a soil sample/layer, instead of encapsulation or bioclogging by crust formation on the soil surface.

The UCS results in this study were compared to previous EICP studies using the urease enzyme. In [13,60], UCS values of approximately 4500 kPa and 4000 kPa were reported, using, respectively, urease enzymes extracted from soybeans and watermelon seeds. It is worth noting that these studies used a different soil type (sand), so the strength values cannot be directly comparable. Moreover, these studies used the ureolytic pathway of biocementation that has been widely investigated and optimised by

many researchers [2–4,61–64]. Thus, despite the lower UCS values recorded in this study, the CA immobilisation and formation of the nanoflower would be a valuable method to stabilise an enzyme for biocementation, as demonstrated.

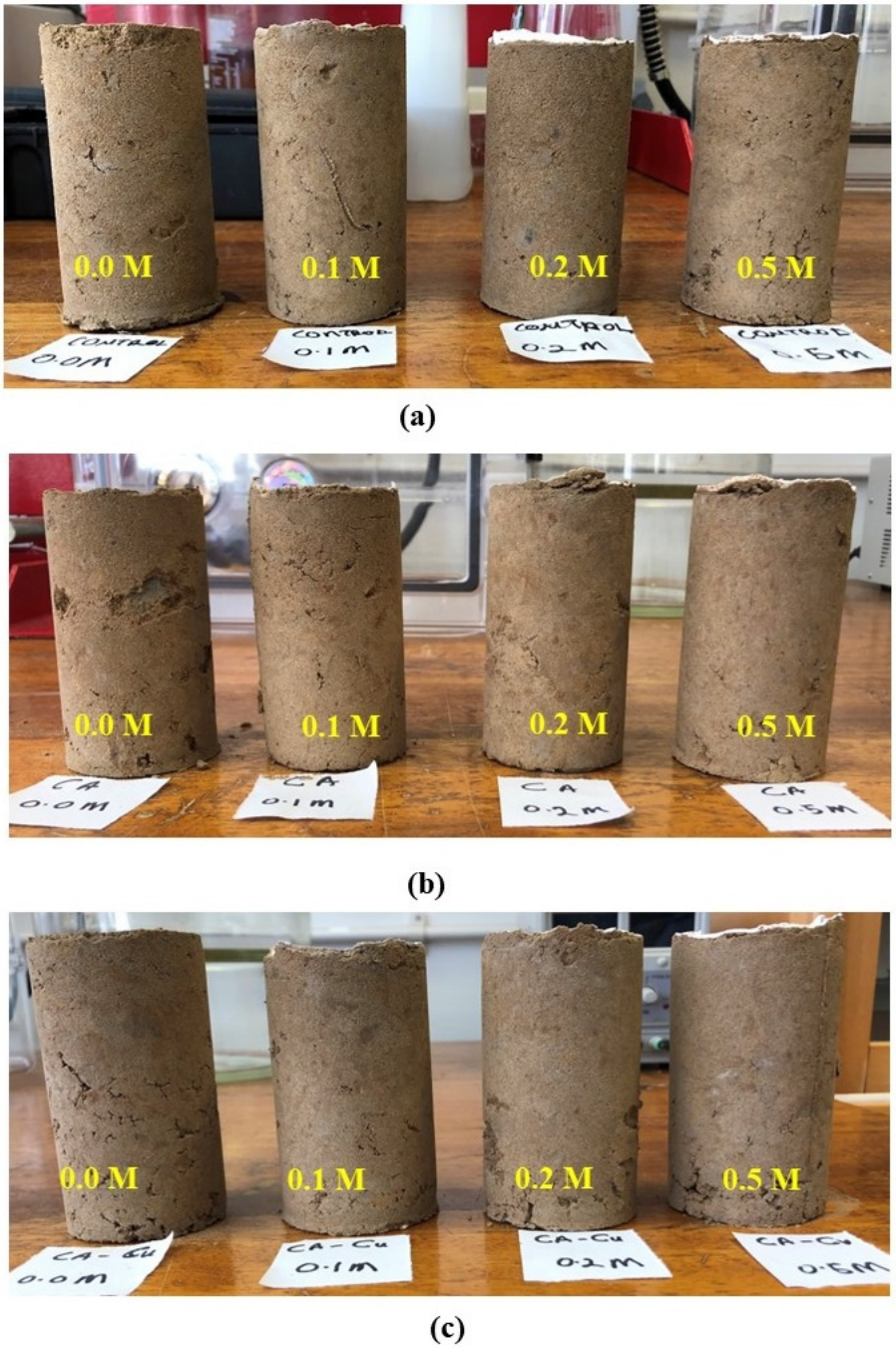


**Figure 9.** The typical appearance of the specimens biocemented by injection (**a**) control, (**b**) biocemented by CA only, and (**c**) biocemented by CA-Cu nanoflower.

### 3.4.2. Calcium Carbonate Content

The precipitated calcium carbonate was measured as it is a critical factor in the increase in the strength of biocemented soil. As with the previously reported results on calcium carbonate distribution for biocementation by injection [65], the amount of calcium carbonate was non-uniform throughout the specimens. High amounts of $CaCO_3$ were observed at the top, compared to the middle and bottom sections of the specimens. This is due to a significantly high reaction rate at the top, leading to bioclogging so that only the upper

soil layers are biocemented. Due to the size of the hybrid carriers, this study did not overcome the uniformity problem; however, had nano-sized carriers been produced, the uniformity challenge could have been addressed. Conversely, the mixing method yielded better uniformity of treatment, with $CaCO_3$ contents ranging between 6% and 10% for the treated samples. As observed, the optimal CA-Cu mixing ratio is 0.1 M, yielding higher UCS and $CaCO_3$ content than a 0.2 M or 0.5 M mixing ratio. Similarly, in most other cases, 0.2 M solutions give higher $CaCO_3$ content and UCS than 0.5 M solutions. Similar observations have been reported in urease enzyme reactions where a highly concentrated solution was undesirable [66].

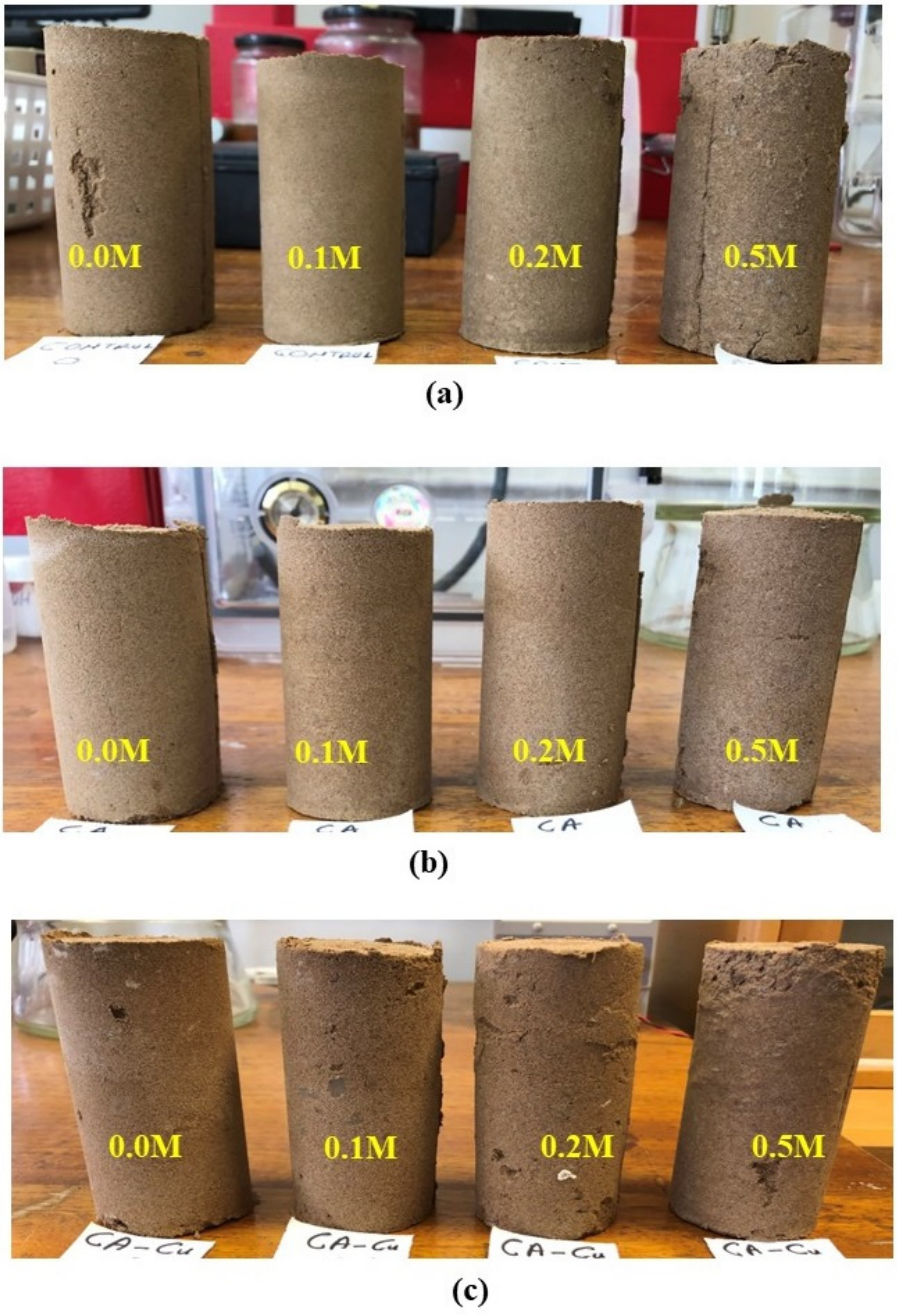


**Figure 10.** The typical appearance of the specimens biocemented by mixing (**a**) control, (**b**) biocemented by CA only, and (**c**) biocemented by CA-Cu nanoflower.

**Table 4.** Comparison of the UCS and calcium carbonate content.

| Treatment | Test Category | $CaCl_2/NaHCO_3$(g) | CA Enzyme Concentration (mg/mL) | $q_u$, (kPa) | Average $CaCO_3$ (%) | Moisture Content (%) |
|---|---|---|---|---|---|---|
| Mixing | Control | 0.0 M | 0 | 11 | 5% | 30 |
| | | 0.1 M | 0 | 100 | 6% | 30 |
| | | 0.2 M | 0 | 108 | 6% | 30 |
| | | 0.5 M | 0 | 108 | 7% | 30 |
| | CA Only | 0.0 M | 0.1 | 109 | 5% | 30 |
| | | 0.1 M | 0.1 | 92 | 6% | 30 |
| | | 0.2 M | 0.1 | 200 | 7% | 30 |
| | | 0.5 M | 0.1 | 189 | 9% | 30 |
| | CA-Cu Nano-flower | 0.0 M | 0.1 | 11 | 5% | 30 |
| | | 0.1 M | 0.1 | 453 | 10% | 30 |
| | | 0.2 M | 0.1 | 387 | 9% | 30 |
| | | 0.5 M | 0.1 | 219 | 8% | 30 |
| Injection | Control | 0.0 M | 0 | 11 | 5% | 30 |
| | | 0.1 M | 0 | 34 | 5% | 30 |
| | | 0.2 M | 0 | 58 | 6% | 30 |
| | | 0.5 M | 0 | 11 | 6% | 30 |
| | CA Only | 0.0 M | 0.1 | 11 | 5% | 30 |
| | | 0.1 M | 0.1 | 44 | 6% | 30 |
| | | 0.2 M | 0.1 | 125 | 12% | 30 |
| | | 0.5 M | 0.1 | 11 | 5% | 30 |
| | CA-Cu Nano-flower | 0.0 M | 0.1 | 11 | 5% | 30 |
| | | 0.1 M | 0.1 | 80 | 6% | 30 |
| | | 0.2 M | 0.1 | 60 | 7% | 30 |
| | | 0.5 M | 0.1 | 34 | 5% | 30 |

Figure 11 shows the SEM results of the biocemented soil. The microphotographs show that the untreated soil had no crystal of $CaCO_3$. Conversely, for the treated specimens, typical $CaCO_3$ crystals on the surface and between particles are observed, consistent with the biocementation mechanism reported in the literature [40,41].

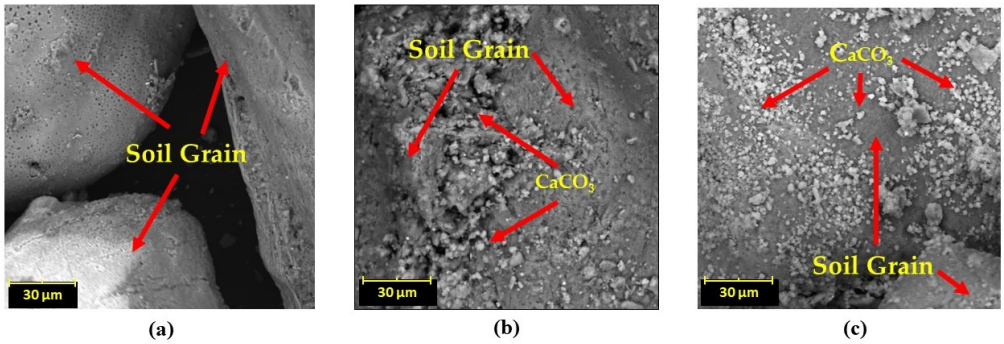


(a) (b) (c)

**Figure 11.** The SEM images of EICP biocemented-treated specimens (**a**) control, (**b**) biocemented by CA only, and (**c**) biocemented by CA-Cu nanoflower.

## 4. Discussion

### 4.1. Anticipated Advantages for Practical Applications

This proof-of-concept study investigated an innovative delivery method of enzymes for biocementation via EICP. The method was applied to a fine-grained soil. For this type of soil, MICP can be a challenge due to the pore throat size compared to bacteria size, and for this reason, EICP was suggested instead. Notably, EICP could also use ex situ produced enzyme by the action of bacteria. However, the main challenge of using free enzymes is the cost of the purified enzyme [67] and its stability in high temperatures and extreme pH conditions [68,69]. The study was conducted to address the stability of the enzyme during EICP treatment using a cheap and easy-to-control protocol. The results were encouraging, as the hybrid carrier enabled the enzyme to maintain 94% of its activity over the study period. This is very promising, as the desired advantage of the proposed delivery method is precisely the long-term stability of the synthesized nanoflowers [25,40,70]. The long-term stability of synthesized nanoflowers can be further investigated at bench scale and field conditions in future research. Such studies can then be used for educated estimates of the cost of the technique in an industrial scale environment, and its overall sustainability in comparison with other soil stabilization methods currently used.

Another advantage is the possibility of recovering and reusing the nanoflower. Reuse and recovery contribute to the sustainability of materials used and the circular economy [71,72]. Therefore, practical ways of recovering the nanoflowers in situ merit further investigation. Moreover, researchers can explore the cost comparison between the suggested and traditional EICP/MICP treatment methods for field applications after establishing ways of nanoflower recovery. As mentioned in the Introduction, for the planned future research by the authors, the recovery of the carriers through an electrokinetic setup will be considered.

Due to their versatility and other advantages discussed in the Introduction, nanoflowers have been used in various biomedical and environmental science applications such as to capture and store or convert and utilize $CO_2$, to diagnose disease biomarkers, biosensors, catalysts, and the therapeutic process along with wastewater remediation and gas sensing [22]. The results from our study proved the hybrid carriers for biocementation for the first time. They indicated that they could play a significant role in enhancing the stability and efficiency of enzymes used for biocementation. The proposed methodology in this study could be thus used for a number of civil and environmental engineering applications of biocementation, such as manufacturing biobricks, enhancing the stability of earthworks and foundation soils, preventing erosion, suppressing dust contamination, or encapsulating and stabilizing pollutants in the soil. Finally, the synthesis of hybrid carriers for other enzymes such as urease [73] or asparaginase [74], which can promote biocementation, could be investigated in future studies.

### 4.2. Limitations of the Presented Experimental Work

Currently, the nanoflowers synthesised in this study were less than 15 μm (see Figure 12). Compared to bacteria whose size could reach 5–6 μm, the macro flowers are too large to penetrate the fine-graded soil as originally desired. This is a limitation of the current work. However, the literature using this type of enzyme carrier for different applications shows that nano-sized carriers can be produced. The successful synthesis of nano-sized carriers of this type requires further experimental work and an improved protocol, as it is sensitive to temperature, pH, buffer solution and metal concentration changes, whose effects should be evaluated further [23,46]. For applying EICP technology in large-scale geotechnical applications, achieving the economical usage of enzymes is essential; the costs of the method at this scale are yet to be determined. Another limitation of this work is that the $CO_2$ captured by the method was not quantitatively measured. This information is of importance to further assess the benefits of the technique in terms of $CO_2$ absorption.

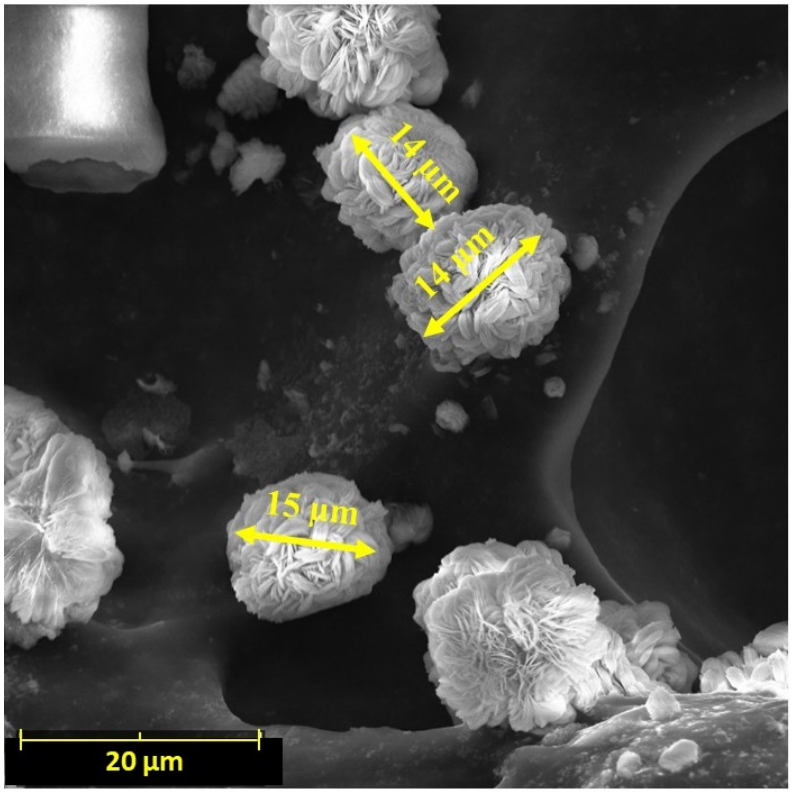


**Figure 12.** SEM image showing the length of CA-Cu hybrid carriers synthesized in this study.

## 5. Conclusions

In this study, we investigated the delivery of immobilized carbonic anhydrase (CA) enzyme in hybrid carriers, as one possible way to overcome the challenges of enzyme instability in the EICP biocementation process. A series of laboratory tests were conducted to fabricate a copper phosphate-based inorganic hybrid enzymatic delivery system that is stable and suitable for biocementation with enhanced enzyme activity and efficiency. The key developments and findings from the study are as follows:

i. The study achieved the synthesis and utilization of inorganic hybrid enzyme carriers with the morphological structure of flowers to biocement soil.
ii. The results showed that the bovine carbonic anhydrase enzyme enhanced the $CO_2$ hydration reaction, resulting in a bioprecipitation reaction and calcium carbonate production. This calcium carbonate was identified as calcite.
iii. The immobilized CA enzyme effectively promoted the absorption of $CO_2$ into the calcium carbonate, which can be used for biocementation with concurrent $CO_2$ sequestration.
iv. It was demonstrated that the immobilised CA enzyme was very stable over long periods of time and within a wide range of pH and temperatures. This result has significant implications for biocementation, as the improved enzyme stability would be helpful in various soil conditions, such as variable temperatures and pH, encountered during ground improvement. The fact that the stability was preserved over months also demonstrates that the hybrid carrier system can promote the reusability of the enzymes.
v. The carriers were successfully used in the soil to achieve biocementation. Their capability as a practical enzyme delivery alternative was demonstrated.
vi. Unconfined compressive strength values of fine-grained soil increased significantly upon implementation of the carriers, especially when mixing was used as a treatment implementation method.

vii. The scanning electron microscope micrographs and Raman spectroscopy confirmed calcite as the primary precipitate formed, which can act as a bonding agent between soil particles to biocement soils.

Thus, the carrier delivery system shows promise that upon further development, enzyme immobilisation can successfully be used for soil biocementation to increase the efficiency and overall sustainability of the EICP process.

**Author Contributions:** W.M., D.P., M.M. and M.J.G., carried out the experiment and analysed the results; W.M., M.M. and D.P. wrote the manuscript with support from M.J.G.; D.P., M.M. and M.J.G. supervised the project; M.M., D.P. and M.J.G. conceived the original idea. All authors have read and agreed to the published version of the manuscript.

**Funding:** The European Commission funded this work under the Horizon 2020 Marie Skłodowska-Curie Individual Fellowships Grant Number 101025184 Project NOBILIS (Grant holder: London South Bank University).

**Institutional Review Board Statement:** Not applicable.

**Informed Consent Statement:** Not applicable.

**Data Availability Statement:** Data sharing does not apply to this article.

**Acknowledgments:** The authors thank Dr Leonardo Pantoja-Muñoz for conducting the SEM-EDS and Raman analyses, Matthew Billing for conducting the XRD analyses and Alejandra Gonzalez for the technical assistance.

**Conflicts of Interest:** The authors declare no conflict of interest.

## References

1. De Jong, J.T.; Soga, K.; Kavazanjian, E.; Burns, S.; van Paassen, L.A.; Al Qabany, A.; Aydilek, A.; Bang, S.S.; Burbank, M.; Caslake, L.F.; et al. Biogeochemical processes and geotechnical applications: Progress, opportunities and challenges. *Géotechnique* **2013**, *63*, 287–301. [CrossRef]
2. Venda Oliveira, P.J.; Freitas, L.D.; Carmona, J.P.S.F. Effect of Soil Type on the Enzymatic Calcium Carbonate Precipitation Process Used for Soil Improvement. *J. Mater. Civ. Eng.* **2016**, *29*, 04016263. [CrossRef]
3. Safdar, M.U.; Mavroulidou, M.; Gunn, M.J.; Garelick, J.; Payne, I.; Purchase, D. Innovative methods of ground improvement for railway embankment peat fens foundation soil. *Géotechnique* **2021**, *71*, 985–998. [CrossRef]
4. Safdar, M.U.; Mavroulidou, M.; Gunn, M.J.; Purchase, D.; Gray, C.; Payne, I.; Garelick, J. Towards the Development of Sustainable Ground Improvement Techniques—Biocementation Study of an Organic Soil. *Circ. Econ. Sustain.* **2022**, *2*, 1589–1614. [CrossRef]
5. Wang, Z.; Su, J.; Ali, A.; Yang, W.; Zhang, R.; Li, Y.; Zhang, L.; Li, J. Chitosan and carboxymethyl chitosan mimic biomineralization and promote microbially induced calcium precipitation. *Carbohydr. Polym.* **2022**, *287*, 119335. [CrossRef]
6. Robles-Fernández, A.; Areias, C.; Daffonchio, D.; Vahrenkamp, V.C.; Sánchez-Román, M. The Role of microorganisms in the nucleation of carbonates, environmental implications and applications. *Minerals* **2022**, *12*, 1562. [CrossRef]
7. Graddy, C.M.; Gomez, M.G.; DeJong, J.T.; Nelson, D.C. Native bacterial community convergence in augmented and stimulated ureolytic MICP biocementation. *Environ. Sci. Technol.* **2021**, *55*, 10784–10793. [CrossRef]
8. Gao, Y.; Wang, L.; He, J.; Ren, J.; Gao, Y. Denitrification-based MICP for cementation of soil: Treatment process and mechanical performance. *Acta Geotech.* **2022**, *17*, 3799–3815. [CrossRef]
9. Jin, P.; Zhang, S.; Liu, Y.; Zhang, W.; Wang, R. Application of Bacillus mucilaginosus in the carbonation of steel slag. *Appl. Microbiol. Biotechnol.* **2021**, *105*, 8663–8674. [CrossRef]
10. Ganendra, G.; Wang, J.; Ramos, J.A.; Derluyn, H.; Rahier, H.; Cnudde, V.; Ho, A.; Boon, N. Biogenic concrete protection driven by the formate oxidation by Methylocystis parvus OBBP. *Front. Microbiol.* **2015**, *6*, 786. [CrossRef]
11. Dhami, N.K.; Mukherjee, A.; Reddy, M.S. Micrographical, minerological and nano-mechanical characterisation of microbial carbonates from urease and carbonic anhydrase producing bacteria. *Ecol. Eng.* **2016**, *94*, 443–454. [CrossRef]
12. Arpajirakul, S.; Pungrasmi, W.; Likitlersuang, S. Efficiency of microbially-induced calcite precipitation in natural clays for ground improvement. *Constr. Build. Mater.* **2021**, *282*, 122722. [CrossRef]
13. Shu, S.; Yan, B.; Ge, B.; Li, S.; Meng, H. Factors affecting soybean crude urease extraction and biocementation via Enzyme-Induced carbonate precipitation (EICP) for soil improvement. *Energies* **2022**, *15*, 5566. [CrossRef]
14. Song, C.; Elsworth, D.; Zhi, S.; Wang, C. The influence of particle morphology on microbially induced $CaCO_3$ clogging in granular media. *Mar. Georesour. Geotechnol.* **2021**, *39*, 74–81. [CrossRef]
15. Sun, X.; Miao, L.; Tong, T.; Wang, C. Study of the effect of temperature on microbially induced carbonate precipitation. *Acta Geotech.* **2019**, *14*, 627–638. [CrossRef]

16. Mortensen, B.M.; Haber, M.J.; DeJong, J.T.; Caslake, L.F.; Nelson, D.C. Effects of environmental factors on microbial induced calcium carbonate precipitation. *J. Appl. Microbiol.* **2011**, *111*, 338–349. [CrossRef]
17. Cui, M.; Lai, H.; Hoang, T.; Chu, J. One-phase-low-pH enzyme induced carbonate precipitation (EICP) method for soil improvement. *Acta Geotech.* **2021**, *16*, 481–489. [CrossRef]
18. Almajed, A.; Lateef, M.A.; Moghal, A.A.B.; Lemboye, K. State-of-the-art review of the applicability and challenges of microbial-induced calcite precipitation (MICP) and enzyme-induced calcite precipitation (EICP) techniques for geotechnical and geoenvironmental applications. *Crystals* **2021**, *11*, 370. [CrossRef]
19. Castro-Alonso, M.J.; Montañez-Hernandez, L.E.; Sanchez-Muñoz, M.A.; Macias Franco, M.R.; Narayanasamy, R.; Balagurusamy, N. Microbially induced calcium carbonate precipitation (MICP) and its potential in bioconcrete: Microbiological and molecular concepts. *Front. Mater.* **2019**, *6*, 126. [CrossRef]
20. Sirisha, V.L.; Jain, A.; Jain, A. Chapter Nine—Enzyme Immobilization: An Overview on Methods, Support Material, and Applications of Immobilized Enzymes. *Adv. Food Nutr. Res.* **2016**, *79*, 179–211. [CrossRef]
21. Lee, S.W.; Cheon, S.A.; Kim, M.I.; Park, T.J. Organic–inorganic hybrid nanoflowers: Types, characteristics, and future prospects. *J. Nanobiotechnol.* **2015**, *13*, 54. [CrossRef] [PubMed]
22. Liu, Y.; Ji, X.; He, Z. Organic-inorganic nanoflowers: From design strategy to biomedical applications. *Nanoscale* **2019**, *11*, 17179–17194. [CrossRef] [PubMed]
23. Ge, J.; Lei, J.; Zare, R.N. Protein-inorganic hybrid nanoflowers. *Nat. Nanotechnol.* **2012**, *7*, 428–432. [CrossRef] [PubMed]
24. Cipolatti, E.P.; Silva, M.J.A.; Klein, M.; Feddern, V.; Feltes, M.M.C.; Oliveira, J.V.; Ninow, J.L.; de Oliveira, D. Current status and trends in enzymatic nanoimmobilization. *J. Mol. Catalysis. B Enzym.* **2014**, *99*, 56–67. [CrossRef]
25. Duan, L.; Li, H.; Zhang, Y. Synthesis of hybrid nanoflower-based carbonic anhydrase for enhanced biocatalytic activity and stability. *ACS Omega* **2018**, *3*, 18234–18241. [CrossRef]
26. Kim, H.S.; Hong, S.-G.; Woo, K.M.; Teijeiro Seijas, V.; Kim, S.; Lee, J.; Kim, J. Precipitation-based nanoscale enzyme reactor with improved loading, stability, and mass transfer for enzymatic $CO_2$ conversion and utilization. *ACS Catal* **2018**, *8*, 6526–6536. [CrossRef]
27. Gadikota, G. Carbon mineralization pathways for carbon capture, storage and utilization. *Commun. Chem.* **2021**, *4*, 23. [CrossRef]
28. Talekar, S.; Jo, B.H.; Dordick, J.S.; Kim, J. Carbonic anhydrase for $CO_2$ capture, conversion and utilization. *Curr. Opin. Biotechnol.* **2022**, *74*, 230–240. [CrossRef]
29. Safdar, M.U.; Mavroulidou, M.; Gunn, M.J.; Purchase, D.; Payne, I.; Garelick, J. Electrokinetic biocementation of an organic soil. *Sustain. Chem. Pharm.* **2021**, *21*, 100405. [CrossRef]
30. *BS 1377:1990*; Methods of Test for Soils for Civil Engineering Purposes. Classification Tests. BSI: London, UK, 1990.
31. *ASTM D2974—14*; Standard Test Methods for Moisture, Ash, and Organic Matter of Peat and Other Organic Soils. ASTM International: West Conshohocken, PA, USA, 2014.
32. *BS EN ISO 17892*; Part 2: 2014 Geotechnical Investigation and Testing—Laboratory Testing of Soil—Part 1: Determination of Bulk Density. BSI: London, UK, 2014.
33. *BS EN ISO 17892*; Part 1: 2014 Geotechnical Investigation and Testing—Laboratory Testing of Soil—Part 1: Determination of Water Content. BSI: London, UK, 2014.
34. *BS ISO 10390:2005*; Soil Quality. Determination of pH. BSI: London, UK, 2005.
35. *ASTM D4373-21*; Standard Test Method for Rapid Determination of Carbonate Content of Soils. ASTM International: West Conshohocken, PA, USA, 2021.
36. *BS EN ISO 17892-7:2018*; Geotechnical Investigation and Testing. Laboratory Testing of Soil-Unconfined Compression Test. BSI: London, UK, 2018.
37. Armstrong, J.M.; Myers, D.V.; Verpoorte, J.A.; Edsall, J.T. Purification and properties of human erythrocyte carbonic anhydrases. *J. Biol. Chem.* **1966**, *241*, 5137–5149. [CrossRef]
38. Chakraborty, A.; Samriti; Ruzimuradov, O.; Gupta, R.K.; Cho, J.; Prakash, J. $TiO_2$ nanoflower photocatalysts: Synthesis, modifications and applications in wastewater treatment for removal of emerging organic pollutants. *Environ. Res.* **2022**, *212*, 113550. [CrossRef]
39. Wang, Q.; Chen, Y.; Zhu, R.; Luo, M.; Zou, Z.; Yu, H.; Jiang, X.; Xiong, X. One-step synthesis of Co(OH)F nanoflower based on micro-plasma: As an effective non-enzymatic glucose sensor. *Sens. Actuators B Chem.* **2020**, *304*, 127282. [CrossRef]
40. Shende, P.; Kasture, P.; Gaud, R.S. Nanoflowers: The future trend of nanotechnology for multi-applications. *Artif. Cells Nanomed. Biotechnol.* **2018**, *46* (Suppl. 1), 413–422. [CrossRef]
41. Dastjerdi, R.; Hashemikia, S. Mechanisms and guidelines on the sustainable engineering of self-assembling; nanostars and nanoflowers. *J. Clean. Prod.* **2021**, *312*, 127570. [CrossRef]
42. Gupta, T.; Samriti; Cho, J.; Prakash, J. Hydrothermal synthesis of $TiO_2$ nanorods: Formation chemistry, growth mechanism, and tailoring of surface properties for photocatalytic activities. *Mater. Today Chem.* **2021**, *20*, 100428. [CrossRef]
43. Li, Y.; Fei, X.; Liang, L.; Tian, J.; Xu, L.; Wang, X.; Wang, Y. The influence of synthesis conditions on enzymatic activity of enzyme-inorganic hybrid nanoflowers. *J. Mol. Catal. B Enzym.* **2016**, *133*, 92–97. [CrossRef]
44. Shao, P.; Shen, Y.; Ye, J.; Zhao, J.; Wang, L.; Zhang, S. Shape controlled ZIF-8 crystals for carbonic anhydrase immobilization to boost $CO_2$ uptake into aqueous MDEA solution. *Sep. Purif. Technol.* **2023**, *315*, 123683. [CrossRef]
45. Kharisov, B.I. A Review for Synthesis of Nanoflowers. *Recent Pat. Nanotechnol.* **2008**, *2*, 190–200. [CrossRef]

46. Ren, S.; Chen, R.; Wu, Z.; Su, S.; Hou, J.; Yuan, Y. Enzymatic characteristics of immobilized carbonic anhydrase and its applications in CO2 conversion. *Colloids Surf. B Biointerfaces* **2021**, *204*, 111779. [CrossRef]
47. Patel, S.K.S.; Otari, S.V.; Chan Kang, Y.; Lee, J. Protein–inorganic hybrid system for efficient his-tagged enzymes immobilization and its application in l -xylulose production. *RSC Adv.* **2017**, *7*, 3488–3494. [CrossRef]
48. Zhang, M.; Zhang, Y.; Yang, C.; Ma, C.; Tang, J. Enzyme-inorganic hybrid nanoflowers: Classification, synthesis, functionalization and potential applications. *Chem. Eng. J.* **2021**, *415*, 129075. [CrossRef]
49. Idrees, D.; Shahbaaz, M.; Bisetty, K.; Islam, A.; Ahmad, F.; Hassan, M.I. Effect of pH on structure, function, and stability of mitochondrial carbonic anhydrase VA. *J. Biomol. Struct. Dyn.* **2017**, *35*, 449–461. [CrossRef] [PubMed]
50. Kanbar, B.; Ozdemir, E. Thermal stability of carbonic anhydrase immobilized within polyurethane foam. *Biotechnol. Prog.* **2010**, *26*, 1474–1480. [CrossRef] [PubMed]
51. Luca, V.D.; Vullo, D.; Scozzafava, A.; Carginale, V.; Rossi, M.; Supuran, C.T.; Capasso, C. An α-carbonic anhydrase from the thermophilic bacterium Sulphurihydrogenibium azorense is the fastest enzyme known for the $CO_2$ hydration reaction. *Bioorg. Med. Chem.* **2013**, *21*, 1465–1469. [CrossRef] [PubMed]
52. Giri, A.; Pant, D. $CO_2$ management using carbonic anhydrase producing microbes from western Indian Himalaya. *Bioresour. Technol. Rep.* **2019**, *8*, 100320. [CrossRef]
53. Fasim, A.; More, V.S.; More, S.S. Large-scale production of enzymes for biotechnology uses. *Curr. Opin. Biotechnol.* **2021**, *69*, 68–76. [CrossRef]
54. Li, W.; Chen, W.; Zhou, P.; Zhu, S.; Yu, L. Influence of initial calcium ion concentration on the precipitation and crystal morphology of calcium carbonate induced by bacterial carbonic anhydrase. *Chem. Eng. J.* **2013**, *218*, 65–72. [CrossRef]
55. Pan, L.; Li, Q.; Zhou, Y.; Song, N.; Yu, L.; Wang, X.; Xiong, K.; Yap, L.; Huo, J. Effects of different calcium sources on the mineralization and sand curing of $CaCO_3$ by carbonic anhydrase-producing bacteria. *RSC Adv.* **2019**, *9*, 40827–40834. [CrossRef]
56. Almajed, A.; Tirkolaei, H.K.; Kavazanjian, E.; Hamdan, N. Enzyme Induced Biocementated Sand with High Strength at Low Carbonate Content. *Sci. Rep.* **2019**, *9*, 1135. [CrossRef]
57. Wani, K.M.N.S.; Mir, B.A. An Experimental Study on the Bio-cementation and Bio-clogging Effect of Bacteria in Improving Weak Dredged Soils. *Geotech. Geol. Eng.* **2021**, *39*, 317–334. [CrossRef]
58. Chu, J.; Ivanov, V.; Naeimi, M.; Stabnikov, V.; Liu, H. Optimization of calcium-based bioclogging and biocementation of sand. *Acta Geotech.* **2014**, *9*, 277–285. [CrossRef]
59. Stabnikov, V.; Naeimi, M.; Ivanov, V.; Chu, J. Formation of water-impermeable crust on sand surface using biocement. *Cem. Concr. Res.* **2011**, *41*, 1143–1149. [CrossRef]
60. Dilrukshi, R.; Nakashima, K.; Kawasaki, S. Soil improvement using plant-derived urease-induced calcium carbonate precipitation. *Soils Found.* **2018**, *58*, 894–910. [CrossRef]
61. Cui, M.; Zheng, J.; Zhang, R.; Lai, H. Soil bio-cementation using an improved 2-step injection method. *Arab. J. Geosci.* **2020**, *13*, 1270. [CrossRef]
62. Whiffin, V.S. Microbial $CaCO_3$ Precipitation for the Production of Biocement. Ph.D. Thesis, Murdoch University, Perth, Australia, 2004; pp. 1–162. Available online: http://researchrepository.murdoch.edu.au/399/2/02Whole.pdf (accessed on 1 June 2023).
63. Abo-El-Enein, S.A.; Ali, A.H.; Talkhan, F.N.; Abdel-Gawwad, H.A. Utilization of microbial induced calcite precipitation for sand consolidation and mortar crack remediation. *HBRC J.* **2012**, *8*, 185–192. [CrossRef]
64. Neupane, D.; Yasuhara, H.; Kinoshita, N.; Unno, T. Applicability of Enzymatic Calcium Carbonate Precipitation as a Soil-Strengthening Technique. *ASCE J. Geotech. Geoenviron. Eng.* **2013**, *139*, 2201–2211. [CrossRef]
65. Gowthaman, S.; Yamamoto, M.; Nakashima, K.; Ivanov, V.; Kawasaki, S. Calcium phosphate biocement using bone meal and acid urease: An eco-friendly approach for soil improvement. *J. Clean. Prod.* **2021**, *319*, 128782. [CrossRef]
66. Phua, Y.J.; Røyne, A. Bio-cementation through controlled dissolution and recrystallization of calcium carbonate. *Constr. Build. Mater.* **2018**, *167*, 657–668. [CrossRef]
67. Poźniak, G.; Krajewska, B.; Trochimczuk, W. Urease immobilized on modified polysulphone membrane: Preparation and properties. *Biomaterials* **1995**, *16*, 129–134. [CrossRef]
68. Ahenkorah, I.; Rahman, M.M.; Karim, M.R.; Beecham, S.; Saint, C. A Review of Enzyme Induced Carbonate Precipitation (EICP): The Role of Enzyme Kinetics. *Sustain. Chem.* **2021**, *2*, 92–114. [CrossRef]
69. Zhang, S.; Zhang, Z.; Lu, Y.; Rostam-Abadi, M.; Jones, A. Activity and stability of immobilized carbonic anhydrase for promoting $CO_2$ absorption into a carbonate solution for post-combustion $CO_2$ capture. *Bioresour. Technol.* **2011**, *102*, 10194–10201. [CrossRef] [PubMed]
70. Liang, S.; Wu, X.; Xiong, J.; Zong, M.; Lou, W. Metal-organic frameworks as novel matrices for efficient enzyme immobilization: An update review. *Coord. Chem. Rev.* **2020**, *406*, 213149. [CrossRef]
71. Ghufran, M.; Khan, K.I.A.; Ullah, F.; Nasir, A.R.; Al Alahmadi, A.A.; Alzaed, A.N.; Alwetaishi, M. Circular Economy in the Construction Industry: A Step towards Sustainable Development. *Buildings* **2022**, *12*, 1004. [CrossRef]
72. Norouzi, M.; Chàfer, M.; Cabeza, L.F.; Jiménez, L.; Boer, D. Circular economy in the building and construction sector: A scientific evolution analysis. *J. Build. Eng.* **2021**, *44*, 102704. [CrossRef]

73. Khodadadi Tirkolaei, H.; Javadi, N.; Krishnan, V.; Hamdan, N.; Kavazanjian, E. Crude Urease Extract for Biocementation. *J. Mater. Civ. Eng.* **2020**, *32*, 04020374. [CrossRef]
74. Li, M.; Fu, Q.; Zhang, Q.; Achal, V.; Kawasaki, S. Bio-grout based on microbially induced sand solidification by means of asparaginase activity. *Sci. Rep.* **2015**, *5*, 16128. [CrossRef] [PubMed]